6-2013

Chip Segmentation in Machining: A Study of Deformation Localization Characteristics in Ti6Al4V

Abhijit Chandra
Iowa State University, achandra@iastate.edu

Pavan Karra
Trine University

Adam Bragg
Flint Hills Resources

Jie Wang
Iowa State University

Gap-Yong Kim
Iowa State University, gykim@iastate.edu

Chip Segmentation in Machining: A Study of Deformation Localization Characteristics in Ti6Al4V

Abstract
Chip segmentation by deformation localization is an important process in a certain range of velocities and might be desirable in reducing cutting forces and by improving chips' evacuation, whereas few studies of practical criteria to calculate shear band spacing are available in literature. This paper extends nonlinear dynamics model for chip segmentation by allowing time varying orientation of the shear plane that are pronounced in strain hardening materials. The model extends the non-linear dynamics approach with additional state variables to the Burns and Davies approach. The model is simulated numerically to predict the shear bands of the chip. The numerical simulation of the model is compared with experimental observations and is in agreement with experimental observations in Ti6Al4V. This offers guidance to predict shear band spacing of other materials.

Keywords
deformation, maching, image segmentation

Comments
This is a conference proceeding from *ASME 2013 International Manufacturing Science and Engineering Conference* 1 (2013): doi:10.1115/MSEC2013-1070. Posted with permission.

Proceedings of the ASME 2013 International Manufacturing Science and Engineering Conference
MSEC2013
June 10-14, 2013, Madison, Wisconsin, USA

MSEC2013-1070

CHIP SEGMENTATION IN MACHINING: A STUDY OF DEFORMATION LOCALIZATION CHARACTERISTICS IN TI6AL4V

Abhijit Chandra
Iowa State University
Ames, IA, USA

Pavan Karra
Trine University
Angola, IN, USA

Adam Bragg
Flint Hills Resources
Rosemount, MN, USA

Jie Wang
Iowa State University
Ames, IA, USA

Gap Yong Kim
Iowa State University
Ames, IA, USA

ABSTRACT

Chip segmentation by deformation localization is an important process in a certain range of velocities and might be desirable in reducing cutting forces and by improving chips' evacuation, whereas few studies of practical criteria to calculate shear band spacing are available in literature. This paper extends nonlinear dynamics model for chip segmentation by allowing time varying orientation of the shear plane that are pronounced in strain hardening materials. The model extends the non-linear dynamics approach with additional state variables to the Burns and Davies approach. The model is simulated numerically to predict the shear bands of the chip. The numerical simulation of the model is compared with experimental observations and is in agreement with experimental observations in Ti6Al4V. This offers guidance to predict shear band spacing of other materials.

INTRODUCTION

Machining has been an essential part of manufacturing for the past several decades. Recent trends in increasing machining speed have introduced additional complexity to the machining process. Higher speeds and higher strain rates increase the magnitude and the rate of heating that needs to be removed from the machining zone [1]. This leads to thermo-mechanical instability during the cutting process.

To continue machining at higher speeds, the dynamics of cutting and chip formation has to be properly understood. Numerous cutting models have been proposed in the literature. Some of the first systematic studies of machining were made by Taylor [2]. Mallock [3] was one of the first to study the machining process theoretically [4]. Merchant [5, 6] and Ernst [6] proposed the widely renowned model of chip formation based on concentrated shear deformation mechanism [4]. Piispanen's card model, despite its limitations, has been very useful in comprehending the material removal in the machining process [7]. Oxley developed predictive machining theory, also known as Oxley's theory, for predicting cutting forces, average temperatures, and stresses in orthogonal cutting with the parallel sided shear zone [8]. Johnson and Cook developed a constitutive model subjected to large strains, high strain rates, and high temperatures [9].

The focus later turned to prediction of shear angle, which was initially recorded by photo micrographs. Piispanen worked on prediction of shear angle, which applied force analysis to the primary machining zone [10]. Cook et al. found that the discontinuous chip formation resembled extrusion process with respect to shear concentration [11]. They also found a periodic variation in coefficient of friction that led to discontinuous chip formation. Wright considered the influence of material strength on shear. The model Burns and Davies developed had two state variables, namely stress and temperature [1]. They assumed that the strain rate followed Arrhenius model and went onto analytically derive the condition for instability. In a follow-up paper, they discussed thermo-mechanical oscillations in metal cutting [12]. In both papers the cutting zone was assumed to be a fixed shear plane since the variation of shear angle was not considered in the model.

In recent years, numerical methods have been applied to better understand the process and the formation of shear bands. Numerical simulations focused on the formation and propagation of the adiabatic shear band was performed by Zhou

et al. [14]. However, nonuniform temperature field within shear bands has not been captured in their work. Investigation in the formation and propagation of adiabatic shear bands has been studied numerically and experimentally by Mason and Worswick [15]. Two and three-dimensional analysis have been made on the shear band propagation by Li et al. [16] [17], Bonnet-Lebouvier et al. [18], and Yang et al. [19] through numerical approach. Zhou et al. [20] developed a numerical method for analyzing one dimensional deformation of thermoviscoplastic materials applied to investigate localization in a thermoviscoplastic material of multiple shear bands [21].

The main objective in this study is to extend the non-linear dynamics approach pioneered by Burns and Davies by incorporating the effect of shear angle variations in predicting the shear band separation. The shear plane is an approximation, and to be more accurate, a shear zone with a time varying shear angle needs to be assumed. In addition, a time varying flow stress in Johnson-Cook model has been applied. The subsequent sections describe the experimental procedure undertaken and development of the numerical model with discussion on the criterion applied to calculate the shear band spacing.

NOMENCLATURE

A = material constant
B = material constant
C = material constant
d = depth of cut
E = elastic modulus
h = thickness of shear bands
K = constant
L = contact length
m = material constant
n = material constant
t = time
$\hat{t}$ = non-dimensional variable
T = absolute temperature inside the zone
T_{melt} = physical interpretation of melting point
T_0 = absolute temperature of the material entering the shear zone (room temperature)
$\hat{T}$ = non-dimensional variable
W = width of contact
$\hat{y}$ = non-dimensional variable
Δl=shear band spacing

Greek Symbols

ϕ_0 = predicted shear angle and also the value corresponding to shear of material at σ_0
ϕ = shear angle
$\dot{\phi}$ = rate of change of shear angle
$\hat{\phi}$ = non-dimensional variable
α = rake angle
σ_y = shear yield strength
σ_u = shear strength of severely work hardened material (corresponding to ultimate strength in tension)/ $\sqrt{3}$
σ_0 = yield strength of the non-work-hardened material
$\hat{\sigma}$ = non-dimensional variable
τ = shear stress
$\sum$ = local compressive stress
γ = plastic strain
$\dot{\gamma}^p$ = plastic strain rate in the primary shear zone
$\dot{\gamma}^p_{avg}$ = average plastic strain rate in the primary shear zone
γ^p_0 = reference plastic strain rate
$\hat{\dot{\gamma}}$ = non-dimensional variable
V = cutting speed
v_{chip} = chip velocity
χ = thermal conductivity of the workpiece
ρ = density
c_γ = specific heat capacity at constant elastic configuration
$\hat{\tau}$ = non-dimensional variable
Φ = plastic strain rate divided by average plastic strain rate
ε = strain-rate sensitivity of the material
υ = thermal-softening parameter

EXPERIMENTAL PROCEDURE

Ti6Al4V was turned at linear speeds ranging from 0.2 m/s to 2.5 m/s. For titanium, 2.5 m/s is normally high speed setting. Chip samples were collected at each of six linear speeds. Under a digital microscope, the chips could be inspected for shear band spacing at chip edge viewpoint and face viewpoint (see FIGURE 1 and FIGURE 2).

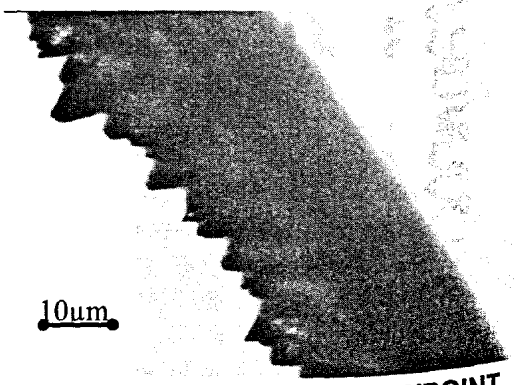

FIGURE 1-CHIP EDGE VIEWPOINT

Under non-orthogonal turning condition, chips were produced in a helical shape. The chip curvature might cause difficulty in viewing the shear plane, but measuring from the chip edge as well as the chip face was quite feasible. FIGURE 1 and FIGURE 2 showed chip viewing orientation examples.

FIGURE 2-CHIP FACE VIEWPOINT

Digital photos of samples viewed under 10x, 50x, and 100x magnification were taken. Each photo of every chip provided several shear band spacing measurements to ensure an appropriate sample size and minima measurement error. Measurements were made peak-to-peak to ensure better accuracy because the valleys of the bands might be unclear and sometimes out of focus. A MATLAB program was used to analyze shear band spacing by converting number of pixels in the digital photos into physical length scale.

Experimental data was also collected to determine the effects of feed rate and shear band spacing. Titanium alloy (Ti6Al4V) was tested under the criteria as outlined for the original cuts. For these tests, however, the feed rate was varied to a maximum value of over eight times that of the original 76 μm/rev. The maximum feed rate was 0.025 in/rev, or roughly 635 μm/rev. Samples were collected and compared for a similar distribution of linear speeds.

MODEL DEVELOPMENT

In the Burns and Davies paper [1], shear angle was assumed to be a constant, and therefore, fixed shear plane could be effectively used for a specific material. In this analysis, however, the constant shear angle assumption is relaxed to approximate a shear zone by incorporating a time varying shear plane approximation. Since the shear angle is no longer constant in time, time varying shear angle is introduced within the dynamic equations [1].

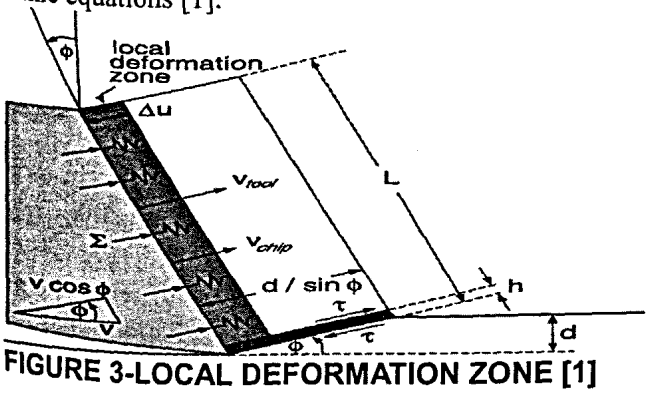

FIGURE 3-LOCAL DEFORMATION ZONE [1]

The shear stress is obtained from the balance of momentum as in FIGURE 3, which is given by [1]:

$$\tau = \frac{\Sigma L W \sin\phi}{Wd} = \frac{EL\sin^2\phi}{d^2}\Delta u$$

$$\Delta u = \frac{\gamma d}{\sin\phi} \tag{1}$$

L is assumed to be the same as undeformed chip thickness d as discussed by Burns and Davies [1]. Taking the derivative to obtain the shear stress rate with shear zone analysis, i.e. the shear angle changes with time; the stress rate is given by:

$$\frac{d\tau}{dt} = \frac{EL\sin^2\phi}{d^2}\left(v\cos\phi - v_{chip}\right) + \frac{EL\sin 2\phi}{d^2}\dot{\phi}\Delta u$$

$$= \frac{ELV\sin^2\phi\cos\phi}{d^2}\left(1 - \frac{\dot{\gamma}^p}{\dot{\gamma}^p_{avg}}\right) + \frac{2EL\cos\phi}{d}\dot{\phi}\gamma \tag{2}$$

The energy equation involving the conduction, convection, heat generation and the temperature decay terms is given by [1]:

$$\frac{dT}{dt} = \frac{T_0 - T}{h}v\sin\phi + \frac{4\chi}{\rho c_\gamma}\frac{T_0 - T}{h^2} + \frac{\tau\dot{\gamma}^p}{\rho c_\gamma} \tag{3}$$

In order to simplify, friction in the secondary zone is neglected as discussed by Burns and Davies [1]. However, it may be achieved by replacing the present modeling with BEM analysis of Chan and Chandra [24]. Kececioglu [22] has experimentally shown that the thickness of the shear band h is around 25 μm over a wide range of materials at various machining conditions. If shear band spacing is small compared to shear band thickness, continuous chips form; if shear band spacing is relatively large comparable to shear band thickness, serrated chips form; if the shear band spacing is much larger than the shear band thickness, the chips become discontinuous.

Wright [13] provided an expression for the shear angle for a work-hardening material as:

$$\cos(\phi_0 - \alpha)\sin\phi_0 = \frac{\sigma_y}{\sigma_u}\cos\left(\frac{\pi}{4} - \frac{\alpha}{2}\right)\sin\left(\frac{\pi}{4} + \frac{\alpha}{2}\right) \tag{4}$$

Differentiating the above expression with respect to time and rearranging the terms, the rate of change of shear angle is given by:

$$\dot{\phi} = \frac{\cos\left(\frac{\pi}{4} - \frac{\alpha}{2}\right)\sin\left(\frac{\pi}{4} + \frac{\alpha}{2}\right)}{\cos(2\phi - \alpha)}\left(\frac{\dot{\sigma}_y}{\sigma_u} - \frac{\sigma_y}{\sigma_u^2}\dot{\sigma}_u\right) \tag{5}$$

On the other hand, the yield strength of a work-hardened material is given by Johnson-Cook model [9]:

$$\sigma_y = \left[A + B\left(\gamma^p\right)^n\right]\left[1 + C\ln\left(\frac{\dot{\gamma}^p}{\dot{\gamma}_0^p}\right)\right]\left[1 - \left(T^*\right)^m\right]$$

$$T^* = \frac{T - T_0}{T_m - T_0} \tag{6}$$

The Johnson-Cook model [9] can be differentiated to obtain the following equation for the derivative of yield strength. The second derivative of plastic strain is negligible compared to other terms. Hence, ignoring the term and assuming that the reference strain rate is the average strain rate $\dot{\gamma}^p_{avg}$, we get:

$$\frac{d\sigma_y}{dt} = [1 + C\ln(\frac{\dot{\gamma}^p}{\dot{\gamma}^p_0})][1 - (T^*)^m][A + nB(\gamma^p)^{n-1}\frac{d\gamma^p}{dt}] \tag{7}$$

$$-[A + B(\gamma^p)^n][1 + C\ln(\frac{\dot{\gamma}^p}{\dot{\gamma}^p_0})]m(T^*)^{m-1}\frac{dT^*}{dt}$$

The equations can be put in the form of four state equations where the state variables are shear strain, shear angle, temperature, and shear stress. The state equations [1] are:

$$\frac{\dot{\gamma}}{\dot{\gamma}^p_{avg}} = e^{\frac{\tau - 1 + \upsilon T}{\varepsilon(1+T)}} \qquad \phi(\tau, T) = e^{\frac{\tau - 1 + \upsilon T}{\varepsilon(1+T)}} \tag{8}$$

The first term of Eq. (8) is the dimensionless plastic strain rate. A phenomenological Arrhenius model is also given in the second part of Eq. (8). Since the plastic flow at high strain rate is thermally activated, Arrhenius kinetics can be applied to this model similarly as in Burns and Davies [1].

The following non dimensional variables are used:

$$\hat{t} = \frac{ELV}{\sigma_0 d^2}t \quad \hat{T} = \frac{T - T_0}{T_0} \quad \hat{y} = \frac{y}{d} \quad \hat{\tau} = \frac{\tau}{\sigma_0}$$

$$\hat{\dot{\gamma}} = \frac{d\gamma}{d\hat{t}} = \frac{\sigma_0 d^2}{ELV}\dot{\gamma}^p_{avg}\Phi \quad \hat{\phi} = \phi \quad \hat{\sigma} = \frac{\sigma}{\sigma_0} \tag{9}$$

Here σ_0 is the yield strength of the non-work-hardened material.

Using the above non-dimensional variables the following equations can be obtained:

$$\frac{d\hat{\gamma}}{d\hat{t}} = \frac{d\gamma}{d\hat{t}} = \frac{\sigma_0 d^2}{ELV}\frac{d\gamma}{dt} = \frac{\sigma_0 d^2}{ELV}\dot{\gamma}^p_{avg}\Phi = \frac{\sigma_0 d^2}{ELV}\dot{\gamma}^p_{avg}e^{\frac{\tau - 1 + \upsilon T}{\varepsilon(1+T)}} \tag{10}$$

Rearranging and simplifying, we get:

$$\frac{d\hat{\phi}}{d\hat{t}} = \frac{\cos\left(\frac{\pi}{4} - \frac{\alpha}{2}\right)\sin\left(\frac{\pi}{4} + \frac{\alpha}{2}\right)}{\cos\left(2\hat{\phi} - \alpha\right)}\left(\frac{\frac{d\hat{\sigma}_y}{d\hat{t}}}{\hat{\sigma}_u} - \frac{\hat{\sigma}_y\frac{d\hat{\sigma}_u}{d\hat{t}}}{\hat{\sigma}_u^2}\right) \tag{11}$$

$$\frac{d\hat{T}}{d\hat{t}} = -\frac{\sigma_0 d^2 \sin\phi}{ELh}\hat{T} - \frac{4\chi\sigma_0 d^2}{\rho c_\gamma ELVh^2}\hat{T} + \frac{\sigma_0}{\rho c_\gamma T_0}\hat{\tau}\frac{d\hat{\gamma}}{d\hat{t}} \tag{12}$$

$$\frac{d\hat{\tau}}{d\hat{t}} = -\frac{\sin^2\hat{\phi}\cos\hat{\phi}}{V}\left(1 - \frac{ELV\dot{\gamma}^p}{\sigma_0 d^2}\right) + \frac{2EL\cos\hat{\phi}}{\sigma_0 d}\frac{d\hat{\phi}}{d\hat{t}}\hat{\gamma} \tag{13}$$

Finally, differentiate the Johnson Cook model's equation by substituting equation (8), we obtain:

$$\frac{d\hat{\sigma}_y}{d\hat{t}} = \left[1 + C\ln\left\{\frac{ELV\dot{\hat{\gamma}}}{\sigma_0 d^2}\right\}\right]\left[1 - \left(K\hat{T}\right)^m\right]nB\left(\gamma^p\right)^{n-1}\frac{\dot{\hat{\gamma}}}{\sigma_0} - \tag{14}$$

$$\left[A + B\left(\gamma^p\right)^n\right]\left[1 + C\ln\left(\frac{ELV\dot{\hat{\gamma}}}{\sigma_0 d^2}\right)\right]m\left(K\hat{T}\right)^{m-1}\frac{KT_0}{\sigma_0}\frac{d\hat{T}}{d\hat{t}}$$

Dropping the hats, the dimensionless non-linear coupled equations become:

$$\dot{\gamma} = \frac{\sigma_0 d^2}{ELV}\dot{\gamma}^p_{avg}e^{\frac{\tau - 1 + \upsilon T}{\varepsilon(1+T)}} \tag{15}$$

$$\dot{\phi} = \frac{\cos\left(\frac{\pi}{4} - \frac{\alpha}{2}\right)\sin\left(\frac{\pi}{4} + \frac{\alpha}{2}\right)}{\cos(2\phi - \alpha)}\left(\frac{\dot{\sigma}_y}{\sigma_u} - \frac{\sigma_y}{\sigma_u^2}\dot{\sigma}_u\right) \tag{16}$$

$$\dot{T} = -\frac{\sigma_0 d^2 \sin\phi}{ELh}T - \frac{4\chi\sigma_0 d^2}{\rho c_\gamma ELVh^2}T + \frac{\sigma_0}{\rho c_\gamma T_0}\tau\dot{\gamma} \tag{17}$$

$$\dot{\tau} = -\frac{\sin^2\phi\cos\phi}{V}\left(1 - \frac{ELV\dot{\gamma}^p}{\sigma_0 d^2}\right) + \frac{2EL\cos\phi}{\sigma_0 d}\dot{\phi}\gamma \tag{18}$$

$$\dot{\sigma}_y = \left[1 + C\ln\left\{\frac{ELV\dot{\gamma}}{\sigma_0 d^2}\right\}\right]\left[1 - (KT)^m\right]nB\left(\gamma^p\right)^{n-1}\frac{\dot{\gamma}}{\sigma_0} \tag{19}$$

$$-\left[A + B\left(\gamma^p\right)^n\right]\left[1 + C\ln\left(\frac{ELV\dot{\gamma}}{\sigma_0 d^2}\right)\right]m(KT)^{m-1}\frac{KT_0}{\sigma_0}\dot{T}$$

γ is obtained by integrating $\dot{\gamma}$ with respect to time.

In this study, the shear band spacing denoted by Δl is calculated through the equation:

$$\Delta l = \frac{d\hat{T}}{d\hat{t}} * \kappa \tag{20}$$

Best fit κ is determined using the least square fitting method over various cutting speeds. In essence, κ depends on thermal characteristics of material, but independent of machining conditions. Local shear instabilities arise from competition between strain hardening and thermal softening. When the cutting velocity is sufficiently low, the cutting process is stable since there is enough time for heat conduction, and therefore, strain hardening will dominate the process. If a

material, however, is deformed rapidly and the time for heat conduction is limited, this process can be effectively regarded as adiabatic for the time-scale of interest and becomes unstable locally. This leads to the formation of the "catastrophic thermoplastic shear bands" in the workpiece material [12]. If conditions give rise to local thermal instability, the shear band spacing will be more distant apart at higher velocities.

RESULTS AND DISCUSSION

Ti6Al4V was simulated using the model described in the previous section with non-linear differential equations. Initially, the state variables were set to zero. Then the derivatives were calculated and then updated after each time step. After data compilation from the experiments, mean spacings were computed for every linear speed with corresponding standard deviations from that mean. The experimental values contained an error bar, which represented the mean value +/- one standard deviation. Table 1 listed the constants used in flow stress model developed by Johnson-Cook for Ti6Al4V [23].

Table 1. Constants of Johnson-Cook model for Ti6Al4V [23]

A[MPa]	B [MPa]	n	C	m
862	331	0.34	0.012	0.8

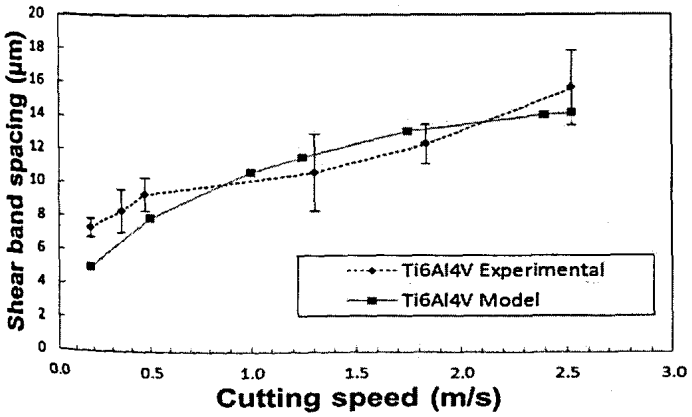

FIGURE 4-TITANIUM MODEL VS EXPERIMENTAL RESULTS AT DIFFERENT VELOCITIES (α = - 5 °, d=75 μm)

As shown in FIGURE 4, experimental and simulated data compared very well for Ti6Al4V. The value of κ in Eq. (20) for Ti6Al4V was 0.94. When compared with simulated results, the material behaved as expected showing increasing shear band spacings with linear speed increments. The trend was decreasing at higher speeds. This again was speculated to be an artifact of the assumption built into the model that all of plastic work was concentrated at the shear plane, and was converted to heat. However, at higher cutting speeds, the net generation rate was higher, and Ti6Al4V being a poor conductor of heat found it very hard to cope with this increased rate of very concentrated heating. This further concentrated the shear band relative to the normalization parameter (federate or chip thickness). At the lower cutting velocities, the simulation results did not capture the mean values of the shear band spacing well and this could be explained as the temperature change was low and compared to the error bars at the higher cutting velocities, the error bars at lower cutting velocities were relatively narrower.

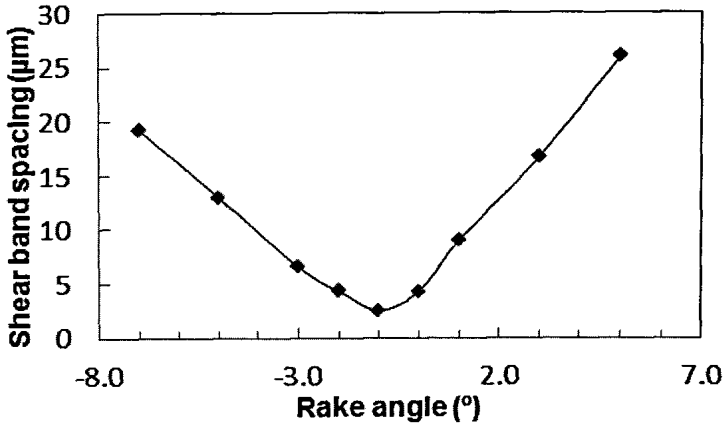

FIGURE 5-EFFECTS OF RAKE ANGLE ON SHEAR BAND SPACING (v=1.75 m/s, d=75 μm)

As shown in FIGURE 5, keeping other cutting conditions constant, the rake angle was varied over a wide range. Increasing the rake angle from -7° initially made the shear band spacing decrease where it reached smallest spacing when the rake angle was -1°. Then, the shear band spacing increased as the rake angle increased again. This result offered guidance as to minimize the shear band spacing in the cutting of Ti6Al4V.

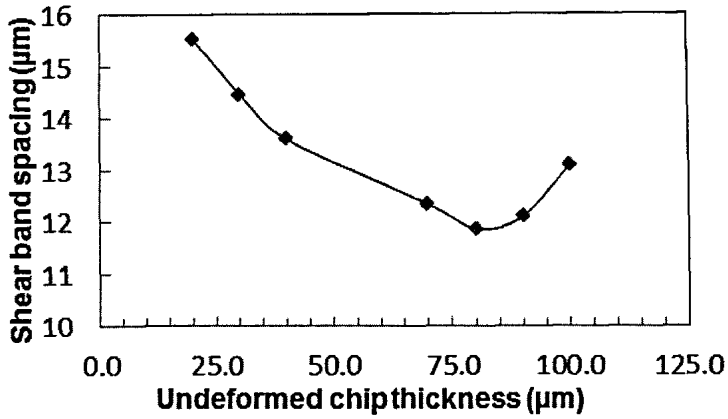

FIGURE 6-EFFECTS OF UNDEFORMED CHIP THICKNESS ON SHEAR BAND SPACING (v=1.75 m/s, α= - 5 °)

Effect of undeformed chip thickness on shear banding spacing was shown in FIGURE 6. Similar to the effects of the rake angle, the minimum shear band spacing could be identified for a given cutting velocity and rake angle. The shear band spacing reached the lowest value when the undeformed chip thickness was around 75 μm.

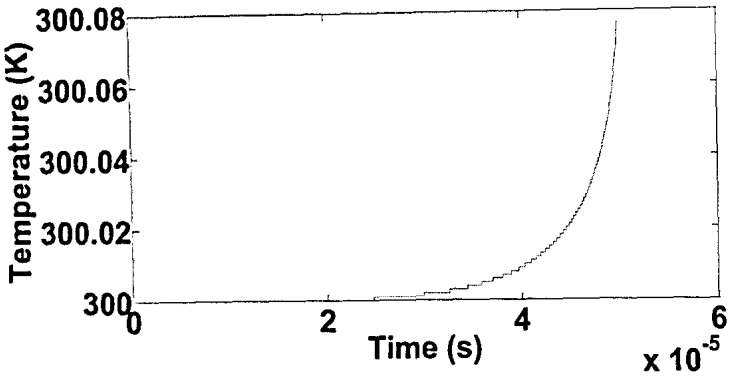

FIGURE 7-TEMPERATURE VARIES WITH TIME (v=1.00 m/s, α= - 5 °, d=30 μm)

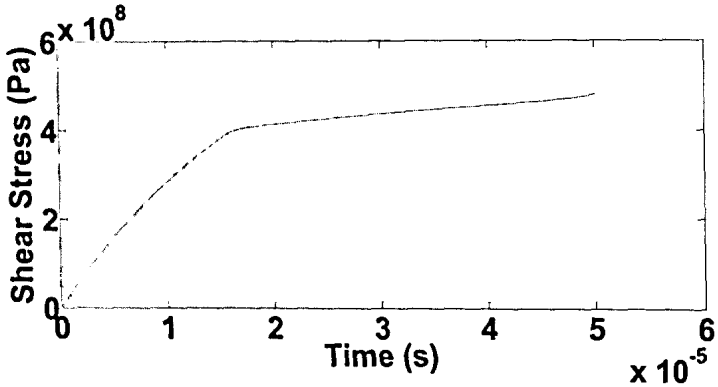

FIGURE 8- SHEAR STRESS VARIES WITH TIME (v=1.00 m/s, α= - 5 °, d=30 μm)

FIGURE 7 and FIGURE 8 showed the variation of temperature and shear stress with time. The primary shear zone deformed rapidly, and plastic energy was generated in a very short time, which led to the rapid increase in temperature. The shear stress initially built up quickly and exceeded the yield stress quickly, which then became stable.

Predicting accurate shear band spacing is critical in understanding chip segmentation phenomenon. Some materials, particularly titanium alloys, form segmented chips where the deformation of the chip is inhomogeneous. Regions of strong and of weak deformation alternate, which leads to a serrated back side of the chip. In general, adiabatic shearing caused by thermo-mechanical instability is to blame for this phenomenon. Strong shear deformation leads to an increase of the temperature in front of the tool tip, and thus weakening the material by thermal softening. The deformation therefore concentrates in this region and causes the formation of narrow, heavily deformed shear bands. Serrated chips act like saw-tooth and are also detrimental to tool life.

CONCLUSIONS

Burns & Davies shear plane model for chip segmentation has been modified by including state variables, shear angle and flow stress. Numerical simulation of Ti6Al4V is performed and compared to the experimental results. Our model simulation results come remarkably close to the experimental results when comparing mean shear band spacing and follow an agreeable trend. The model which has combined nonlinear dynamics, flow stress model and shear zone theory, shear angle variations has the ability to predict near-accurate shear band spacing's in serrated chips which are detrimental to both the tool material and work. The successful predictions provides key insights into possible avenues for analyzing the shear band spacing and we theorize that with accurate material parameters, our model could produce results, that could a long way in predicting the correct process parameters required to reduce or eliminate the conditions that lead to serrated chip formation.

ACKNOWLEDGMENTS

The authors gratefully acknowledge the financial support by the U.S. National Science Foundation under Grant No. CMMI-0640826 and CMMI-0900093. Any opinions, conclusions or recommendations expressed are those of the authors and do not necessarily reflect views of the sponsoring agencies.

REFERENCES

[1] Burns, T. J., Davies, M. A., 1997, "Nonlinear Dynamics Model for Chip Segmentation in Machining", Physical Review Letters, 79(3), pp.447-450.

[2] Taylor, F. W., 1907, "*On the art of cutting metals*", ASME Transactions, New York, 28, pp.310-350.

[3] Mallock, A., 1881, "The action of cutting tools", Proceedings of the Royal Society of London, 33, pp.127-139.

[4] Shaw, M. C., 2005, "*Metal Cutting Principles*", Oxford University Press, New York.

[5] Merchant, M. E., 1945, "Mechanics of the metal cutting process. I. Orthogonal cutting and type 2 chip", Journal of Applied Physics, 16, pp.267-275.

[6] Ernst, H., Merchant, M. E., 1941, "Chip formation, friction and high quality machined surface", Surface Treatment of Metals, 29, pp.299.

[7] Piispanen, V., 1937, "Lastunmuodostumisen Teoriaa", Teknillinen Aiakauslehti, 27(9), pp.315-322.

[8] Oxley, P. L. B., 1989, "*The Mechanics of Machining: An Analytical Approach to Assessing Machinability*", Ellis Horwood Ltd., England.

[9] Johnson, G. R., Cook, W. H., 1983, "*A Constitutive Model and Data for Metals Subjected to Large Strains, High Strain Rates and High Temperatures*", Proceedings: 7th International Symposium on Ballistics, The Hague, The Netherlands, pp.541-547.

[10] Piispanen, V., 1948, "Theory of formation of metal chips", Journal of Applied Physics, 19, pp.876-881.

[11] Cook, N. H., Finnie, I., Shaw, M. C., 1954, "Discontinuous chip formation", ASME Transactions, 76, pp.153-162.

[12] Burns, T. J., Davies, M. A., 2001, "Thermomechanical Oscillations in Material Flow during High-Speed Machining", Philosophical Transaction of the Royal Society A, 359, pp.821-846.

[13] Wright, P. K., 1982, "Predicting the shear plane angle in machining from the work-material strain-hardening characteristics", Journal of Engineering for Industry, 104, pp.285-293.
[14] Zhou, M., Ravichandran, G., Rosakis, A. J., 1996, "Dynamically propagating shear bands in impact-loaded prenotched plates-II.Numerical simulations", Journal of Mechanics and Physics of Solids, 44, pp.1007-1032.
[15] Mason, C., Worswick, M. I., 2001, "Adiabatic shear in annealed and shock-hardened iron and in quenched and tempered 4340 steel", International Journal of Fracture, 111, pp. 29–51.
[16] Li, S., Liu, W. K., Qian, D., Guduru, P. R., Rosakis, A. J., 2001, "Dynamic shear band propagation and micro-structure of adiabatic shear band", Computer Methods Applied Mechanics and Engineering, 191, pp.73-92.
[17] Li, S., Liu, W. K., Rosakis, A. J., Belyschko, T., Hao, W., 2002, "Mesh-free Galerkin simulations of dynamic shear band propagation and failure mode transition", International Journal of Solids Structure, 39, pp. 1213–1240.
[18] Bonnet-Lebouvier, A.-S., Molinari, A., Lipinski, P., 2002, "Analysis of the dynamic propagation of adiabatic shear bands", International Journal of Engineering Science, 39, pp. 4249–4269.
[19] Yang, Q., Mota, A., Ortiz, M., 2005, "A class of variational strain-localization finite elements", International Journal for Numerical Methods in Engineering, 62, pp. 1013–1037.
[20] Zhou, F., Wright, T. W., Ramesh, K. T., 2006, "A numerical methodology for investigating the formation of adiabatic shear bands", Journal of the Mechanics and Physics of Solids, 54(5), pp.904-926.
[21] Zhou, F., Wright, T. W., Ramesh, K. T., 2006, "The formation of multiple adiabatic shear bands", Journal of the Mechanics and Physics of Solids, 54(7), pp.1376-1400.
[22] Kececioglu, D., 1958, "*Shear strain rate in metal cutting and its effects on shear flow stress*", ASME Transactions, New York, 80, pp. 158
[23] Donald, R. L., 2000, "Experimental Investigations of Material Models for Ti-6Al-4V Titanium and 2024-T3 Aluminum", DOT/FAA/AR-00/25, National Technical Information Service, Springfield, Virginia.
[24] Chan, C. L., Chandra, A., 1991, "A Boundary Element Method Analysis of the Thermal Aspects of Metal Cutting Processes", Journal of Engineering for Industry, 113(3), pp.311-319.